

## Detection of furcation involvement using periapical radiography and 2 cone-beam computed tomography imaging protocols with and without a metallic post: An animal study

Fernanda Cristina Sales Salineiro<sup>1</sup>, Ivan Onone Gialain<sup>1</sup>, Solange Kobayashi-Velasco<sup>1</sup>,  
Claudio Mendes Pannuti<sup>1</sup>, Marcelo Gusmão Paraiso Cavalcanti<sup>1,\*</sup>

<sup>1</sup>Department of Stomatology, School of Dentistry, University of São Paulo, São Paulo, Brazil

### ABSTRACT

**Purpose:** The purpose of this study was to assess the accuracy, sensitivity, and specificity of the diagnosis of incipient furcation involvement with periapical radiography (PR) and 2 cone-beam computed tomography (CBCT) imaging protocols, and to test metal artifact interference.

**Materials and Methods:** Mandibular second molars in 10 macerated pig mandibles were divided into those that showed no furcation involvement and those with lesions in the furcation area. Exams using PR and 2 different CBCT imaging protocols were performed with and without a metallic post. Each image was analyzed twice by 2 observers who rated the absence or presence of furcation involvement according to a 5-point scale. Receiver operating characteristic (ROC) curves were used to evaluate the accuracy, sensitivity, and specificity of the observations.

**Results:** The accuracy of the CBCT imaging protocols ranged from 67.5% to 82.5% in the images obtained with a metallic post and from 72.5% to 80% in those without a metallic post. The accuracy of PR ranged from 37.5% to 55% in the images with a metallic post and from 42.5% to 62.5% in those without a metallic post. The area under the ROC curve values for the CBCT imaging protocols ranged from 0.813 to 0.802, and for PR ranged from 0.503 to 0.448.

**Conclusion:** Both CBCT imaging protocols showed higher accuracy, sensitivity, and specificity than PR in the detection of incipient furcation involvement. Based on these results, CBCT may be considered a reliable tool for detecting incipient furcation involvement following a clinical periodontal exam, even in the presence of a metallic post. (*Imaging Sci Dent 2017; 47: 17-24*)

**KEY WORDS:** Cone-Beam Computed Tomography; Furcation Defects; Diagnosis; Radiography, Dental

### Introduction

Furcation involvement is defined as the “pathologic resorption of bone within a furcation,”<sup>1</sup> and is the result of a progression of periodontal disease into the interradicular area of molar teeth. Furcation involvement may be classified as class I (incipient lesions), corresponding

to periodontal loss of less than 3 mm between the buccal and lingual surfaces of the root; class II, defined as periodontal loss of 3 mm or greater, but not exceeding the whole distance between the buccal and lingual surfaces of the root; and class III, exhibiting total loss of periodontal/bone tissue in the furcation area.<sup>2</sup>

Furcation involvement is considered to be one of the most important prognostic factors for the loss of molars.<sup>3,4</sup> Treatment of furcation involvement represents a challenge to clinicians due to the anatomy of the furcation<sup>5,6</sup> and the limited physical access to the area. Therefore, it is often appropriate for early manifestations of these lesions to be evaluated and managed by a periodontist.

\*This study was funded by CNPq (National Council for Research, Brasilia, Brazil), the Universal Research Project (grant no. 472895/2009-5), and a Research Productivity Scholarship (grant no. 303847/2009-3).

Received June 15, 2016; Revised September 19, 2016; Accepted October 31, 2016

\*Correspondence to : Prof. Marcelo Gusmão Paraiso Cavalcanti

Department of Stomatology, Avenida Professor Lineu Prestes, 2227, 05508-000, Cidade Universitária, São Paulo, SP, Brazil  
Tel) 55-11-3091-7807, Fax) 55-11-3091-7807, E-mail) mgpcaval@usp.br

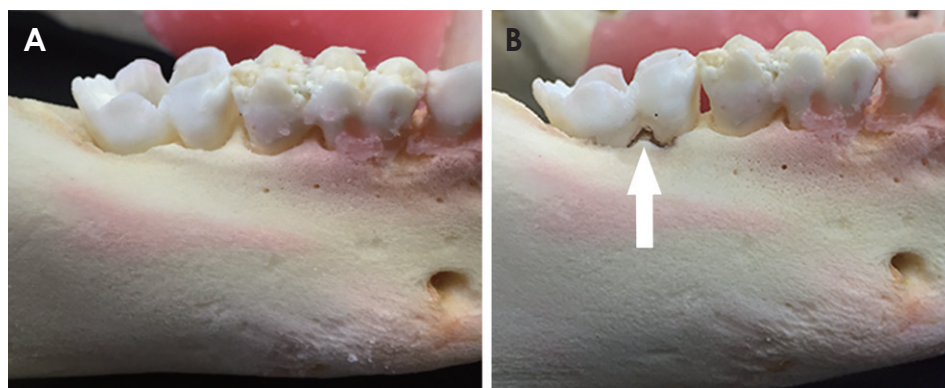


**Fig. 1.** The pig mandibles before (A) and after (B) the chemical lesions were simulated (arrow).

Proper diagnosis of furcation involvement is essential for the definition of an appropriate treatment plan and the establishment of prognosis of the involved tooth. Traditionally, the gold standard diagnosis of furcation involvement is based on clinical examination with a Nabers probe and the imaging method applied is periapical radiography (PR).<sup>7</sup>

PR is a 2-dimensional imaging technique. This form of exam might not be accurate enough for the assessment of furcation involvement, mainly as a result of image overlay and a consequent lack of sufficient information.<sup>8</sup>

Cone-beam computed tomography (CBCT) is another imaging modality that can be used in dentistry. CBCT imaging provides a 3-dimensional image, without superimposition of anatomic structures. This exam is commonly used in dentistry because of its high diagnostic accuracy<sup>9,10</sup> and high image quality.

One of the most frequent limitations in using CBCT for diagnostic purposes is the presence of a metallic artifact. Endodontically treated teeth present intracanal metallic posts, and dental implants may produce artifacts in CBCT images.<sup>11</sup> These artifacts are represented by radiopaque, radiolucent, and bright tracks that can overlap the teeth<sup>12</sup> or bone and mimic bone loss.<sup>13</sup> Previous studies have compared images in which metallic posts are present or absent,<sup>11,12</sup> different metallic post compositions,<sup>14</sup> metallic and fiber posts,<sup>15</sup> and PR or CBCT imaging for tooth fracture diagnosis.<sup>16</sup> In all studies, the artifacts created by the presence of the posts reduced the diagnostic accuracy of the observers.

Thus, the aim of this study was to assess the accuracy, sensitivity, and specificity of the diagnosis of incipient furcation involvement (class I) with the presence or absence of intracanal metallic posts, comparing PR and 2 different CBCT imaging protocols in macerated pig mandibles.

## Materials and Methods

### Selection of specimens

This study was submitted to the Ethics and Research Committee of our institution and approved under protocol no. 104/2010. Ten dry mandibles of young adult domestic pigs were used. Before the simulated lesions were created, the specimens were clinically assessed and CBCT images were analyzed to evaluate whether they had any original bone defect that could be misinterpreted in the ensuing diagnostic imaging exam.<sup>17,18</sup> If a specimen had an original bone defect, it was excluded from the study.

### Simulating bone lesions in the furcation region

Simulated lesions were created in the furcation region of both mandibular second molars in the buccal or lingual aspects of the bone (Fig. 1), in order to blind the observer on the location of the bone lesion.

One of the authors applied a 2-mm cotton pellet soaked in 70% perchloric acid (Merck Chemicals, Darmstadt, Germany), in order to create furcation lesions. The pellets were kept in contact with the bone for 2 hours. After each application, the mandibles were washed for 1 minute under tap water to remove all perchloric acid from the bone, according to a methodology used in previous studies.<sup>13,17,18</sup> Lesions up to one-third of the lingual-buccal distance of the second molar furcation<sup>19</sup> were created to simulate incipient bone loss caused by periodontal disease at an early stage.

Afterwards, a cobalt-chromium metallic post was inserted into either the buccal or the lingual root canal. If the simulated lesion was created in the buccal aspect of the bone, the metallic post was inserted into the buccal root canal; the same methodology was applied for the lingual root canal.

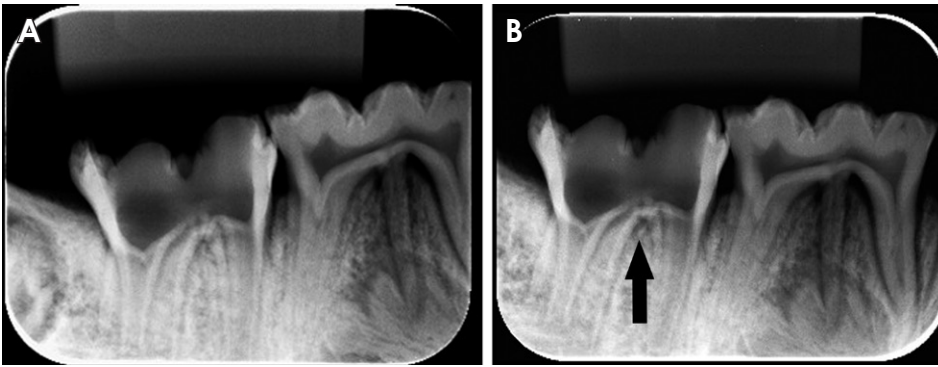


**Fig. 2.** Periapical radiographs without a lesion (A), and with a lesion (B), illustrating the difficulty in identifying the lesion on periapical radiographs. The lesion is indicated by the arrow in the area where it was created.

### Image acquisition

The same co-author who created the furcation lesions performed the CBCT and PR imaging of the mandibles. The CBCT images were acquired using ProMax 3D Max (Planmeca, Helsinki, Finland). Two acquisition protocols were selected for this study: (1) standard, with 96 kVp, 12 mA, 400 frames (number of projections), a 5-cm × 5.5-cm cylindrical field of view (FOV), a 0.2-mm voxel size, and 10.8 mGy (value given by the machine); and (2) high definition (HD), with 96 kVp, 12 mA, 500 frames (number of projections), a 5-cm × 5.5-cm cylindrical FOV, a 0.15-mm voxel size, and 13.7 mGy (value given by the machine). The CBCT images were obtained with the axial plane oriented parallel to the mandible base, simulating the position that would be used in a clinical setting.

Digital periapical radiographs were acquired using a size 2 (31-mm × 41-mm) digital photostimulable phosphor plate (Digora, Soredex, Milwaukee, WI, USA) aligned parallel to the second molar and taken with an intraoral X-ray machine (Dabi Atlante, Ribeirão Preto, Brazil) with exposure settings of 70 kVp, 7 mA, and 0.4 seconds. In each case, the object-to-source distance was 30 cm.

The imaging acquisitions were performed on 2 different occasions: before the lesion simulation (control group, n = 20) and after the lesion simulation (test group, n = 20). Thus, an equal number of CBCT images and periapical radiographs of second molars with a mesiopalatal canal were obtained. In all situations, a 2-cm-thick wax plate was placed in the mandible to attenuate the X-ray beam and promote soft tissue equivalence.

### Periapical and CBCT image evaluation

Two blind observers with experience in interpreting CBCT images and periapical radiographs were trained and calibrated on the radiographic and tomographic features of furcation involvement. They were not involved in the process of creating the lesions and in the imaging

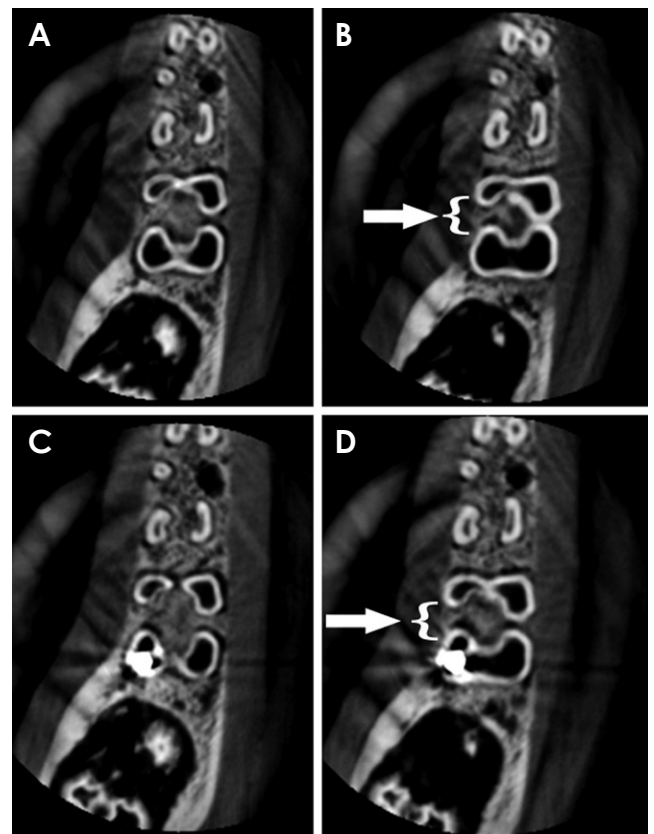


**Fig. 3.** CBCT standard imaging protocol in axial images without a metallic post and without a lesion (A), without a metallic post and with a lesion (B, arrow with brace), with a metallic post and without a lesion (C), and with a metallic post and with a lesion (D, arrow with brace). CBCT, cone-beam computed tomography.

acquisition.

The observers were asked to assess the mandibular second molar region and to identify the absence or presence of furcation involvement. They analyzed the periapical radiographs and the reconstructed CBCT images (axial, coronal, and sagittal, simultaneously) using a basic viewer from OsiriX MD 1.2 (64-bit, Pixmeo, Geneva, Switzer-

**Table 1.** Sensitivity, specificity, and accuracy of the analysis of furcation involvement

		HD protocol			Standard protocol			Periapical radiograph		
		Se	Sp	Ac	Se	Sp	Ac	Se	Sp	Ac
With a metallic post	Obs. 1.1	78.0%	60.0%	67.5%	60.0%	85.0%	72.5%	65.0%	35.0%	50.0%
	Obs. 1.2	75.0%	85.0%	80.0%	70.0%	75.0%	72.5%	65.0%	45.0%	55.0%
	Obs. 2.1	85.0%	80.0%	82.5%	75.0%	90.0%	82.5%	45.0%	50.0%	47.5%
	Obs. 2.2	65.0%	80.0%	72.5%	65.0%	80.0%	72.5%	25.0%	50.0%	37.5%
Without a metallic post	Obs. 1.1	80.0%	65.0%	72.5%	65.0%	75.0%	70.0%	55.0%	55.0%	55.0%
	Obs. 1.2	80.0%	80.0%	80.0%	75.0%	70.0%	72.5%	70.0%	55.0%	62.5%
	Obs. 2.1	80.0%	70.0%	75.0%	85.0%	70.0%	77.5%	40.0%	45.0%	42.5%
	Obs. 2.2	65.0%	65.0%	65.0%	70.0%	80.0%	75.0%	30.0%	55.0%	42.5%

HD, high definition; Obs. observer; Se, sensitivity; Sp, specificity; Ac, accuracy

land). They used all the software visualization tools (contrast, magnification, and window width and level) (Figs. 2 and 3). The observers were then asked to rate the absence or presence of furcation involvements according to a 5-point scale (1 = definitely absent, 2 = probably absent, 3 = uncertain, 4 = probably present, 5 = definitely present) assessed in each of the 10 mandibles with and without a metallic post.

A second assessment of the same images using the same rating procedure was repeated within a 14-day interval by the same observers, in order to determine the reproducibility of the observations.

#### Data analysis

Statistical analysis was carried out using the kappa test (SPSS version 17.0.0; SPSS Inc., Chicago, IL, USA). The values for the kappa coefficient ( $\kappa$ ) were calculated to assess intraobserver and interobserver agreement, which were classified according to the following criteria: slight agreement, 0.0-0.20; fair agreement, 0.21-0.40; moderate agreement, 0.41-0.60; good agreement, 0.60-0.80; excellent agreement, 0.81-1.00.<sup>20</sup>

The sensitivity, specificity, and accuracy of the 2 CBCT imaging protocols and PR were calculated, with and without the presence of the metallic post. All the responses were tabulated with the criterion standard (obtained through a visual analysis of the macerated mandible) and plotted into a web-based calculator for receiver operating characteristic (ROC) curves.<sup>13</sup>

The areas under the ROC curves (AUC) in the protocols were compared by using the Mann-Whitney test (Wilcoxon Rank-Sum test), adopting  $p \leq .05$  as the cut-off for statistical significance (Bioestat version 5.3, Instituto Mamirauá, Tefé, Brazil).

## Results

Table 1 shows the individual values of sensitivity, specificity, and accuracy for each observer in both observations (1 and 2) in each image type. For the HD protocol, the accuracy ranged from 67.5% to 82.5% in the images with a metallic post and from 72.5% to 80% in the images without a metallic post. For the standard protocol, the accuracy ranged from 72.5% to 82.5% in the images with a metallic post and from 72.5% to 77.5% in the images without a metallic post. The accuracy of PR ranged from 37.5% to 55% in the images with a metallic post and from 42.5% to 62.5% in the images without a metallic post. The values for the CBCT images were higher than the values for the periapical radiographs.

Table 2 shows the individual and averaged observers' AUC values with respect to the image type used. For the detection of furcation defects, the HD protocol ( $AUC = 0.802 \pm 0.072$ ) provided detection rates equal to the standard protocol ( $AUC = 0.804 \pm 0.015$ ) and a higher detection rate than PR ( $AUC = 0.448 \pm 0.172$ ) in the samples with a metallic post. For the samples without a metallic post, the trends were similar among the HD protocol ( $AUC = 0.813 \pm 0.048$ ), the standard protocol ( $AUC = 0.789 \pm 0.030$ ), and PR ( $AUC = 0.503 \pm 0.214$ ). In the presence of a metallic post, the AUC values of both CBCT imaging protocols were significantly higher than those of the periapical radiographs. The HD protocol was significantly superior to periapical radiographs in the absence of a metallic post. There was no significant difference between the standard protocol and periapical radiographs in the absence of a metallic post. Furthermore, there was no significant difference between the CBCT imaging protocols, with or without a metallic post.

The interobserver and intraobserver agreement values

**Table 2.** The area under the receiver operating characteristic curve for furcation involvement with and without a metallic post

	With a metallic post			Without a metallic post		
	HD protocol	Standard protocol	Periapical radiograph	HD protocol	Standard protocol	Periapical radiograph
Obs. 1.1	0.741	0.806	0.511	0.82	0.753	0.542
Obs. 1.2	0.789	0.823	0.662	0.819	0.803	0.779
Obs. 2.1	0.908	0.785	0.343	0.866	0.779	0.424
Obs. 2.2	0.773	0.805	0.279	0.748	0.824	0.27
Mean (SD)	0.802 (0.072)	0.804 (0.015)	0.448 (0.172)	0.813 (0.048)	0.789 (0.030)	0.503 (0.214)
Mann-Whitney Values						
<i>P</i> -value	HD protocol vs. periapical radiograph		Standard protocol vs. periapical radiograph		HD protocol vs. standard protocol	
With a metallic post	0.02*		0.02*		0.38	
Without a metallic post	0.04*		0.06		0.56	

HD, high definition; Obs., observer; SD, standard deviation

**Table 3.** Kappa values for intraobserver and interobserver agreement

Kappa	HD protocol		Standard protocol		Periapical radiograph	
	Without a metallic post	With a metallic post	Without a metallic post	With a metallic post	Without a metallic post	With a metallic post
Obs. 1 × Obs. 1	0.4	0.35	0.84	0.69	0.49	0.59
Obs. 2 × Obs. 2	0.45	0.45	0.65	0.59	0.45	0.25
Obs. 1 × Obs. 2	0.5	0.54	0.35	0.49	0.03	0

HD, high definition; Obs. observer

are shown in Table 3. The kappa value ranged from fair to moderate (0.35 to 0.54) for the HD protocol, fair to excellent (0.35 to 0.84) for the standard protocol, and slight to moderate (0 to 0.59) for the periapical radiographs.

## Discussion

The early diagnosis of a furcation defect is paramount in determining the treatment plan for the tooth, as diagnosis can prevent eventual tooth loss. For this reason, furcation defect class I (incipient lesions) were chosen for the present study. Incipient lesions always precede furcation defects and must be identified first through a clinical periodontal exam<sup>21</sup> and confirmed using CBCT imaging.<sup>22</sup> A clinical periodontal exam is important for identifying the suspect area of the lesion and determining the area to be scanned. The chosen CBCT imaging protocol should be one with a small FOV, covering only the region of interest. This imaging modality provides better information on the size, shape, and location of the lesion when compared to a periapical radiograph. These data can provide valuable information for clinical diagnosis, helping in treat-

ment planning,<sup>18</sup> and may aid in the avoidance of redundant surgical or endodontic interventions.<sup>23</sup> Furthermore, periapical radiographs, also included in this study, may serve as a supplementary procedure to the clinical examination.<sup>7,21</sup>

Pigs are considered a good animal model to represent the human craniofacial region for study. Their anatomy, morphology, and bone density in this region are similar to those of humans. This makes swine mandible bone a good sample material for radiological studies.<sup>24,25</sup>

Umetsubo et al.<sup>18</sup> developed the methodology for simulating chemical bone lesions in the furcation region. However, in our study, periapical radiographs were added to compare the results with those of the CBCT exam. Our accuracy levels (67.5% to 82.5%) were similar to those of other study authors (78% to 88%), which demonstrates the efficacy of CBCT.

The diagnosis accuracy ranged from 65% to 82.5% for the HD protocol and from 70% to 82.5% for the standard protocol. These accuracy values showed no significant difference between CBCT imaging with or without metallic artifact, suggesting that, for incipient furcation in-

involvement, CBCT imaging can be accurately used as a diagnostic tool even in the presence of a metallic intracanal post, as demonstrated in Figure 3.

Graetz et al.<sup>4</sup> analyzed bone loss using PR exams and panoramic radiographs. The performance of these 2 imaging exam protocols did not show sufficient accuracy. Therefore, the authors suggested combining clinical and radiographic evaluations. In our study, the accuracy in PR exams ranged from 37.5% to 62.5%. A PR exam results in an inherent superimposition of other structures<sup>12</sup> such as the cortical bone and anatomic structures, which complicates the visualization of furcation defects. In our research, PR showed serious limitations in diagnosing furcation defects, and the imaging accuracy was lower than CBCT. These results reflect the limitations of 2-dimensional exams. Bone defects and furcation involvement are usually better depicted with CBCT imaging than with PR.<sup>26</sup> Bone lesion observation with a PR image of 2-rooted or 3-rooted teeth is complicated, since an eventual superimposition of anatomic structures<sup>27</sup> and the thickness of cortical bone can influence the visualization of the images.<sup>28</sup>

Qiao et al.<sup>29</sup> performed measurements to investigate the accuracy of CBCT imaging in assessing maxillary molar furcation involvement and compared this to results obtained at the time of furcation surgery. The CBCT and intrasurgical assessments presented a strong agreement.<sup>29</sup> Our findings accord with those results. CBCT demonstrated high accuracy in assessing the loss of periodontal tissue in areas with incipient furcation involvement and in the classification of furcation involvement. Although our study was conducted in animals, the CBCT results obtained in this clinical study for the diagnosis of furcation involvement were accurate.

There are different acquisition and post-acquisition protocols for CBCT imaging. Specific characteristics of different CBCT imaging protocols may influence the quality of a computed tomographic scan and the radiation dosage delivered to the patient.<sup>30</sup> In this study, 2 different CBCT imaging protocols were used: HD and standard. Each protocol had a different voxel size, number of frames, and acquisition time; however, the FOV size for both protocols was equal.

The appropriate selection of CBCT acquisition parameters in the postoperative assessment of the images for diagnosis is important for determining image quality and the radiation dose.<sup>13</sup> The selected FOV size, voxel thickness, number of frames, kVp, and mA can directly influence CBCT image quality, with implications for specific

diagnoses.<sup>9,13,27</sup>

These parameters influenced the signal-to-noise ratio. In our study, we used a small FOV and the 2 smallest voxel sizes available in the CBCT scan to analyze the furcation area and obtained good results in both protocols. Accordingly, Salineiro et al.<sup>11</sup> observed that proportional FOV and voxel size resulted in better diagnosis results.

The 2 protocols used in this study were similar in confirming furcation defects. Both protocols attained high levels of sensitivity, specificity, and accuracy, while the comparison among the AUCs showed no statistically significant difference between the CBCT imaging protocols, and the kappa values for the standard protocol were excellent. Thus, these results suggest that the higher radiation dose in the HD protocol may be an unnecessary patient risk, given that the standard protocol resulted in an equally high accuracy level using a smaller radiation dose. According to the “as low as reasonably achievable” (ALARA) principle, it is better to obtain radiographic images with enough quality at the lowest possible radiation dose to the patient. Therefore, the CBCT standard imaging protocol with a small FOV has sufficient quality for furcation involvement diagnosis at a lower dose than the HD protocol.

Artifact strikes have a negative influence in CBCT images. In the presence of metallic posts, sensitivity, specificity, and accuracy levels decreased 5.0% in comparison to furcation defects without a metallic post using both CBCT and PR exams. In CBCT imaging, the influence of metallic artifacts was minimal. This must have occurred due to the distance between the object that caused the artifact and the furcation area. Benic et al.<sup>31</sup> reported a decrease in artifact strike intensity when the distance from the object that caused the interference increased. In PR images, the metallic post did not overlap the furcation region.

Aljehany et al.<sup>26</sup> analyzed 3 different voxel sizes for the assessment of periodontal furcation involvement. The authors concluded that larger voxel size reduced the accuracy of the assessment of periodontal furcation involvement, but not to a significant extent. This study did not use the full range of CBCT volume to make a diagnosis; 6 images of each tooth were selected for the observers. The image selection could induce bias in this study, because the observer already had the best images of the lesion.

In conclusion, both CBCT imaging protocols showed higher accuracy, sensitivity, and specificity than periapical radiographs in the detection of incipient furcation involvement, even in the presence of a metallic post. Based

on these results, CBCT can be considered a reliable aid to clinical periodontal examination in the detection of incipient furcation involvement.

### Acknowledgements

The authors thank the Coordination of the Advancement of Higher Education (CAPES), Brasília, Brazil (a PhD fellowship grant to Fernanda Salineiro and Ivan Gialain) and CNPq, Brasília, Brazil (an MA fellowship grant to Solange Velasco).

### References

1. American Academy of Periodontology. Glossary of periodontal terms. 4th ed. Chicago: American Academy of Periodontology; 2001.
2. Hamp SE, Nyman S, Lindhe J. Periodontal treatment of multirooted teeth. Results after 5 years. *J Clin Periodontol* 1975; 2: 126-35.
3. Dannewitz B, Zeidler A, Hüsing J, Saure D, Pfefferle T, Eichholz P, et al. Loss of molars in periodontally treated patients: results 10 years and more after active periodontal therapy. *J Clin Periodontol* 2016; 43: 53-62.
4. Graetz C, Schützhold S, Plaumann A, Kahl M, Springer C, Sälzer S, et al. Prognostic factors for the loss of molars - an 18-years retrospective cohort study. *J Clin Periodontol* 2015; 42: 943-50.
5. Bower RC. Furcation morphology relative to periodontal treatment. Furcation entrance architecture. *J Periodontol* 1979; 50: 23-7.
6. Svärdröm G, Wennström JL. Furcation topography of the maxillary and mandibular first molars. *J Clin Periodontol* 1988; 15: 271-5.
7. Mol A. Imaging methods in periodontology. *Periodontol* 2000 2004; 34: 34-48.
8. Cimbajevic MM, Spin-Neto RR, Miletic VJ, Jankovic SM, Aleksic ZM, Nikolic-Jakoba NS. Clinical and CBCT-based diagnosis of furcation involvement in patients with severe periodontitis. *Quintessence Int* 2015; 46: 863-70.
9. Cavalcanti MG. Cone beam computed tomographic imaging: perspective, challenges, and the impact of near-trend future applications. *J Craniofac Surg* 2012; 23: 279-82.
10. De Vos W, Casselman J, Swennen GR. Cone-beam computerized tomography (CBCT) imaging of the oral and maxillofacial region: a systematic review of the literature. *Int J Oral Maxillofac Surg* 2009; 38: 609-25.
11. Salineiro FC, Pinheiro LR, dos Santos Junior O, Cavalcanti MG. Detection of horizontal root fracture using four different protocols of cone-beam computed tomography. *Braz Oral Res* 2015; 29. pii: S1806-83242015000100264.
12. Costa FF, Gaia BF, Umetsubo OS, Cavalcanti MG. Detection of horizontal root fracture with small-volume cone-beam computed tomography in the presence and absence of intracanal metallic post. *J Endod* 2011; 37: 1456-9.
13. Pinheiro LR, Scarfe WC, Augusto de Oliveira Sales M, Gaia BF, Cortes AR, Cavalcanti MG. Effect of cone-beam computed tomography field of view and acquisition frame on the detection of chemically simulated peri-implant bone loss in vitro. *J Periodontol* 2015; 86: 1159-65.
14. Mohammadpour M, Bakhshalian N, Shahab S, Sadeghi S, Ataee M, Sarikhani S. Effect of titanium and stainless steel posts in detection of vertical root fractures using NewTom VG cone beam computed tomography system. *Imaging Sci Dent* 2014; 44: 89-94.
15. Ferreira RI, Bahrami G, Isidor F, Wenzel A, Haiter-Neto F, Groppo FC. Detection of vertical root fractures by cone-beam computerized tomography in endodontically treated teeth with fiber-resin and titanium posts: an in vitro study. *Oral Surg Oral Med Oral Pathol Oral Radiol* 2013; 115: e49-57.
16. Takeshita WM, Iwaki LC, da Silva MC, Sabio S, Albino PR. Comparison of periapical radiography with cone beam computed tomography in the diagnosis of vertical root fractures in teeth with a metallic post. *J Conserv Dent* 2014; 17: 225-9.
17. Santos Junior O, Pinheiro LR, Umetsubo OS, Cavalcanti MG. CBCT-based evaluation of integrity of cortical sinus close to periapical lesions. *Braz Oral Res* 2015; 29. pii: S1806-83242015000100216.
18. Umetsubo OS, Gaia BF, Costa FF, Cavalcanti MG. Detection of simulated incipient furcation involvement by CBCT: an in vitro study using pig mandibles. *Braz Oral Res* 2012; 26: 341-7.
19. Glickman I. Clinical periodontology: the periodontium in health and disease. 2nd ed. Philadelphia, PA: W.B. Saunders; 1958. p. 694-6.
20. Landis JR, Koch GG. The measurement of observer agreement for categorical data. *Biometrics* 1977; 33: 159-74.
21. Laky M, Majdalani S, Kapferer I, Frantal S, Gahleitner A, Moritz A, et al. Periodontal probing of dental furcations compared with diagnosis by low-dose computed tomography: a case series. *J Periodontol* 2013; 84: 1740-6.
22. Walter C, Weiger R, Zitzmann NU. Periodontal surgery in furcation-involved maxillary molars revisited - an introduction of guidelines for comprehensive treatment. *Clin Oral Investig* 2011; 15: 9-20.
23. Bowers GM, Schallhorn RG, McClain PK, Morrison GM, Morgan R, Reynolds MA. Factors influencing the outcome of regenerative therapy in mandibular Class II furcations: Part I. *J Periodontol* 2003; 74: 1255-68.
24. Štembírek J, Kyllar M, Putnová I, Stehlík L, Buchtová M. The pig as an experimental model for clinical craniofacial research. *Lab Anim* 2012; 46: 269-79.
25. Wang S, Liu Y, Fang D, Shi S. The miniature pig: a useful large animal model for dental and orofacial research. *Oral Dis* 2007; 13: 530-7.
26. Aljehani YA. Diagnostic applications of cone-beam CT for periodontal diseases. *Int J Dent* 2014; 2014: 865079.
27. Costa FF, Gaia BF, Umetsubo OS, Pinheiro LR, Tortamano IP, Cavalcanti MG. Use of large-volume cone-beam computed tomography in identification and localization of horizontal root fracture in the presence and absence of intracanal metallic post. *J Endod* 2012; 38: 856-9.
28. Barbat J, Messer HH. Detectability of artificial periapical

- lesions using direct digital and conventional radiography. *J Endod* 1998; 24: 837-42.
29. Qiao J, Wang S, Duan J, Zhang Y, Qiu Y, Sun C, et al. The accuracy of cone-beam computed tomography in assessing maxillary molar furcation involvement. *J Clin Periodontol* 2014; 41: 269-74.
30. Costa FF, Pinheiro LR, Umetsubo OS, dos Santos O Jr, Gaia BF, Cavalcanti MG. Influence of cone-beam computed tomographic scan mode for detection of horizontal root fracture. *J Endod* 2014; 40: 1472-6.
31. Benic GI, Sancho-Puchades M, Jung RE, Deyhle H, Hämerle CH. In vitro assessment of artifacts induced by titanium dental implants in cone beam computed tomography. *Clin Oral Implants Res* 2013; 24: 378-83.